Colloid Polym Sci (2005) 283: 1100–1107
DOI 10.1007/s00396-004-1260-7

Eri Yoshida
Motonari Tanaka
Toshikazu Takata

Self-assembly control of a pyridine-containing diblock copolymer by perfluorinated counter anions during salt-induced micellization

Received: 17 September 2004
Accepted: 10 November 2004
Published online: 11 June 2005

E. Yoshida (✉)
Department of Materials Science, Toyohashi University of Technology, 1-1, Hibarigaoka, Tempaku-cho, Toyohashi, Aichi 441-8580, Japan
E-mail: eyoshida@tutms.tut.ac.jp
Tel.: +81-532-446814

M. Tanaka
Department of Polymer Science and Engineering, Kyoto Institute of Technology, Goshokaido-cho, Matsugasaki, Sakyo, Kyoto 606-8585, Japan

T. Takata
Department of Organic and Polymeric Materials, Tokyo Institute of Technology O-okayama, Meguro-ku, Tokyo 152-8552, Japan

Abstract The micelle formation of poly[(4-pyridinemethoxymethyl)styrene]-*block*-polystyrene (PPySt-*b*-PSt) was studied in the nonselective solvent using perfluoroalkyl carboxylic acids. PPySt-*b*-PSt showed no self-assembly into micelles in THF, because this solvent was nonselective for the copolymer. Dynamic light scattering demonstrated that the diblock copolymer formed the micelles in the solvent in the presence of perfluoroalkyl carboxylic acids in which the number of carbons in the perfluoroalkyl chains was over eight. ^{1}H NMR revealed that the micellization proceeded through the salt formation of the pyridinium perfluoroalkyl carboxylate and through the aggregation of the perfluoroalkyl chains in the counter anions. The hydrodynamic radius and the aggregation number of the micelles increased with an increase in the length of the perfluoroalkyl chain. The copolymer needed less carboxylic acid with longer perfluoroalkyl chain to form the micelles. The copolymer produced the micelles with lower aggregation number and higher critical micelle concentration at higher temperature, although the micellar size was almost independent of the temperature. The micelles were unstable with respect to the variation in the temperature, and were dissociated into the unimers with the increase in the temperature. The micelles, however, were reconstructed by decreasing the temperature. This dissociation–reconstruction of the micelles was controlled reversibly not only by the temperature but also by the concentration of the perfluoroalkyl carboxylic acid. An increase in the acid concentration suppressed the dissociation into the unimers, while promoting the reconstruction of the micelles.

Key words Poly[(4-pyridinemethoxymethyl)styrene]-*block*-polystyrene (PPySt-*b*-PSt) · Perfluoroalkyl carboxylic acid · Micelles hydrodynamic radius · Aggregation number

Introduction

Micelle formation induced by variation in the surroundings and interaction has received scientific attention in recent years, because the methods of the micelle formation can control the self-assembly of macromolecules. The macromolecules are ordinary block and/or random copolymers. The variation in the surroundings is often caused by changes in temperature, pressure, and pH. The micelle formation induced by temperature [1–4] or pressure [5–9] is based on the difference in the solubility of the blocks composing the block copolymers through the changes in these factors. In the pH-induced micelle formation, protonation–deprotonation in parts

of a block copolymer controls the self-assembly [10–12]. The interaction between parts of a block copolymer with other compounds also manipulates the self-assembly [13–15]. The micelle formation is a salt-induced micellization.

While amphiphilic copolymers form micelles by direct self-assembly, in the induced micellization, nonamphiphilic copolymers molecularly and completely dissolved in solvents form the micelles through conversion of the nonamphiphilic copolymers into amphiphilic ones in situ by the variation in the surroundings and interaction. The indirect micelle formation has advantages over the direct micellization in that a variety of amphiphilic copolymers can be created from a nonamphiphilic copolymer in situ by selecting factors that can vary the surroundings and the kind of interaction. The advantages include the fact that there is no dependence on the balance of solvophilic and solvophobic moieties when designing the copolymers.

Pyridine-containing block copolymers are often used for the micelle formation induced by pH [16, 17] and salt formation [18, 19]. The pyridine moieties serve as proton acceptors in the pH-induced micellization and as ligands of metal complexes in the salt-induced micellization [20, 21]. We found that a nonamphiphilic diblock copolymer consisting of poly[(4-pyridinemethoxymethyl)styrene] (PPySt) and polystyrene (PSt) formed micelles in the presence of perfluoroalkyl carboxylic acids and that the self-assembly of the copolymer was controlled by the length of the perfluoroalkyl chain. This paper describes the light scattering studies concerning micelle formation of the poly[(4-pyridinemethoxymethyl)styrene] -*block*-polystyrene diblock copolymer (PPySt-*b*-PSt) by perfluoroalkyl carboxylic acid. The thermal response of the micelles is also described.

Experimental

Instrumentation

^{1}H NMR spectra were obtained with Bruker ARX-500 and JEOL GSX-500 FT NMR spectrometers. Light scattering experiments were performed with a Photal Otsuka Electronics DLS-7000 super dynamic light scattering spectrometer equipped with an LS-71 control unit, an LS-72 pump controller, and an argon ion laser operating at $\lambda = 488$ nm.

Materials

4-Methoxy-2,2,6,6-tetramethylpiperidine-1-oxyl (4-methoxy-TEMPO) was prepared as reported previously [22]. Benzoyl peroxide (BPO) was precipitated from chloroform and recrystallized in methanol at 0 °C. Commercial grade styrene was washed with aqueous alkaline solution and water and distilled over calcium hydride. Sodium hydride was washed with hexane several times and dried in vacuum just before use. DMF was distilled over calcium hydride. THF was purified by refluxing on and distilling over sodium. 4-Chloromethylstyrene and 4-pyridinemethanol were used without further purification. Extrapure tridecafluoroheptanoic acid (Pf-6), pentadecafluorooctanoic acid (Pf-7), heptadecafluorononanoic acid (Pf-8), nonadecafluorodecanoic acid (Pf-9), perfluoroundecanoic acid (Pf-10), perfluorododecanoic acid (Pf-11), and perfluorotetradecanoic acid (Pf-13) were purchased from the Aldrich Chemical Co. or Daikin Chemicals Sales, Ltd., and were used without further purification.

Synthesis of 4-(pyridinemethoxymethyl)styrene (PySt)

A solution of 4-pyridinemethanol (7.51 g, 68.8 mmol) in DMF (20 mL) was added a suspended solution of NaH (2.48 g, 103 mmol) in DMF (70 mL) at 0 °C. The mixture was stirred at room temperature for 45 min. A solution of 4-chloromethylstyrene (7.00 g, 45.9 mmol) in DMF (15 mL) was added to the mixture at 0 °C, and the mixture was stirred at room temperature for 15 h. After the reaction, 200 mL of ether was added to the mixture and washed with water several times. The ether layer was dried with anhydrous magnesium sulfate, and evaporated to remove the ether, dried in vacuum for several hours. The crude product (10.39 g) was obtained. PySt was separated by a silica gel column with benzene/ethyl acetate = 1/1 (vol/vol) as the eluent. PySt (7.73 g) was obtained as yellow liquid. ^{1}H NMR ($CDCl_3$, ppm): δ 4.58 (2H, s, O-C H_2-pyridine), 4.61 (2H, s, O-C H_2-styrene), 5.28 (1H, d, $J = 11$ Hz, vinyl C H), 5.79 (1H, d, $J = 18$ Hz, vinyl C H), 6.75 (1H, dd, $J =$ 11, 18 Hz, vinyl C H), 7.30 (2H, d, $J = 5$ Hz, C H, 3-pyridyl), 7.36 (2H, d, $J = 8$ Hz, C H, 3-styryl), 7.44 (2H, d, $J = 8$ Hz, C H, 2-styryl), 8.60 (2H, d, $J =$ 5 Hz, C H, 2-pyridyl).

Synthesis of PPySt-*b*-PSt

PySt (2.09 g, 9.28 mmol), BPO (37 mg, 0.153 mmol), and 4-methoxy-TEMPO (40 mg, 0.215 mmol) were placed in ampule. After the contents were degassed, the ampule was sealed in vacuum. The polymerization was carried out at 125 °C for 7.5 h and was terminated by cooling with liquid nitrogen. The reaction mixture was dissolved in dichloromethane and poured into hexane to precipitate PPySt. The polymer was purified by repeated reprecipitation from dichloromethane into hexane. The precipitate was then dried in vacuum for several hours to obtain PPySt (1.67 g). The PPySt prepolymer (887 mg)

and styrene (3.64 g, 34.9 mmol) were placed in ampule. After the contents were degassed, the ampule was sealed in vacuum. The polymerization was carried out at 125 °C for 48 h. The reaction mixture was dissolved in dichloromethane and poured into methanol to precipitate the resulting polymer. The polymer was precipitated repeatedly from dichloromethane into methanol to remove the PPySt prepolymer remained. The precipitate was then dried in vacuum for several hours to obtain PPySt-*b*-PSt (2.57 g).

Light scattering measurements: general procedure

PPySt-*b*-PSt (10 mg) was dissolved in THF (3 mL), and using a syringe, the resulting solution was injected through a microporous filter into a cell. The solution was subjected to light scattering measurement at 20 °C. After the measurement, 8 μL of solution of Pf-11 (227.5 mg, 0.370 mmol) in THF (0.5 mL) was added to the copolymer solution in the cell, and the mixture was shaken vigorously. The solution was allowed to stand at 20 °C for 10 min, then subjected to light scattering again. This procedure was repeated until distribution due to the unimers disappeared completely in nonnegatively constrained least-squares (NNLS) analysis [23].

Results and discussion

The PPySt-*b*-PSt diblock copolymer was prepared through the living radical polymerization mediated by 4-methoxy-TEMPO (Fig. 1). The molecular weight of the PPySt prepolymer was Mn = 12,000 by ^{1}H NMR analysis using the signal intensities of two different kinds of the methylene protons for the PySt units and the methoxy protons for 4-methoxy-TEMPO attached to the polymer chain end. The ^{1}H NMR spectrum of the PPySt prepolymer is shown in Fig. 2. The proton signals of the methylene were observed at 4.45 ppm, while the signals of the methoxy at 3.2–3.4 ppm. The signals at 0.8–1.2 ppm also originated from 4-methoxy-TEMPO. Those were based on the tetramethyl group. The signals at 8.60 and 7.18 ppm were attributed to the protons located at the 2 and 3 positions on the pyridine moiety, respectively. The molecular weight distribution of the PPySt prepolymer could not be determined by GPC, because the polymer was adsorbed on polystyrene gels in the columns with THF as the eluent. Figure. 2 also shows the ^{1}H NMR spectrum of the PPySt-*b*-PSt diblock copolymer. The molecular weight of the copolymer was determined using the signal intensities of the methylene protons at 4.45 ppm and the aromatic protons at 6.1–7.3 ppm. The molecular weight was Mn(PPySt-*b*-PSt) = 12,000-*b*-33,000.

Poly[(4-pyridinemethoxymethyl)styrene]-*block*-polystyrene shows no micellization in THF, because the solvent is nonselective for the copolymer. Dynamic light scattering demonstrated that the PPySt-*b*-PSt copolymer formed micelles in the solvent in the presence of perfluoroalkyl carboxylic acids. Figure. 3 shows the variation in hydrodynamic radii and aggregation numbers of the copolymer during the micellization using Pf-6, Pf-7, Pf-8, Pf-9, Pf-10, Pf-11, and Pf-13. We represented the aggregation number as relative aggregation number estimated from the relative scattering intensity (I/I_0). This is because the copolymer concentration is immutable during the micellization and the interaction between the pyridinium moiety and the perfluoroalkyl carboxylic acids without aggregation has no effect on the scattering intensity. It supports the pertinence of this estimation that the addition of trifluoroacetic acid to the copolymer solution had no changes in the hydrodynamic radius and the scattering intensity of the copolymer. Accordingly, the relative scattering intensity may be regarded as apparent aggregation numbers estimated approximately. The copolymer formed micelles in the presence of the perfluoroalkyl carboxylic acids in which the number of carbons in the perfluoroalkyl chains was over eight. The hydrodynamic radius of the micelles increased as a result of increasing the length of the perfluoroalkyl chains. The transition from the unimers to the micelles was shifted to the lower side of the molar ratio of the perfluoroalkyl carboxylic acid to the PySt unit (PfCOOH/PySt) with an increase in the number of perfluoroalkyl carbons. The copolymer needed less

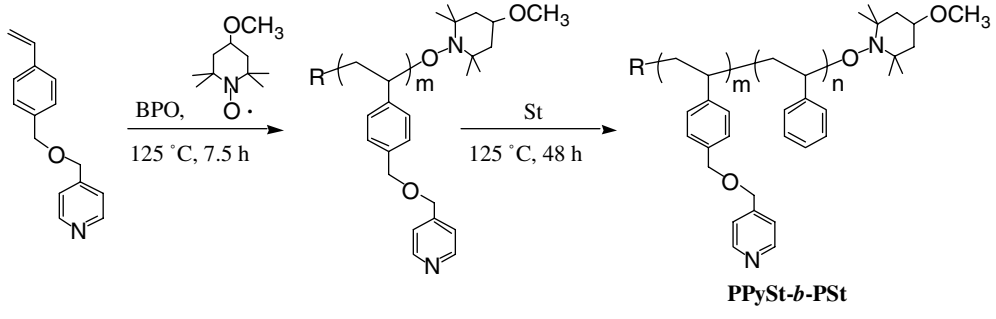

Fig. 1 Synthesis of the PPySt-*b*-PSt diblock copolymer

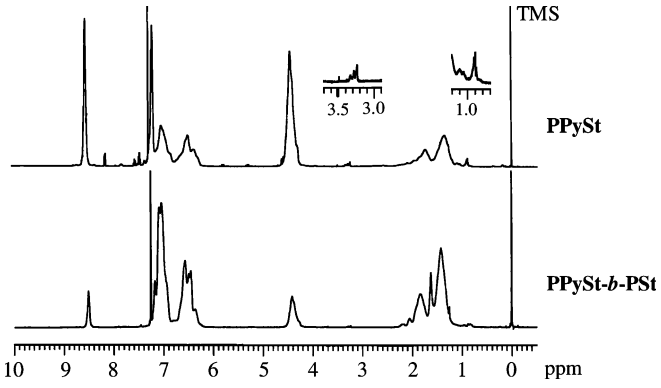

Fig. 2 ^{1}H NMR spectra of the PPySt prepolymer and the PPySt-*b*-PSt block copolymer. Solvent: $CDCl_3$

carboxylic acid for longer perfluoroalkyl chains to produce the micelles. The carboxylic acid with a longer perfluoroalkyl chain had a stronger aggregation force, resulting in the production of the micelles at a lower PfCOOH/PySt ratio. The strength of the aggregation force based on the perfluoroalkyl chain was reflected in the aggregation number of the micelles. The aggregation number at the complete micellization increased with an increase in the length of the perfluoroalkyl chain. We deduced that the length of the perfluoroalkyl chain determined the micellar size and the aggregation number.

Figure 4 shows the variability in the distribution of the hydrodynamic radius of the copolymer during the micellization by Pf-11. The distribution was obtained by the NNLS analysis. The copolymer exists as unimers in the absence of the perfluoroalkyl carboxylic acid. The distribution of the unimers was observed at around a 9-nm hydrodynamic radius. When Pf-11 was added to the copolymer solution (Pf-11/PySt = 2.5), another distribution was discerned around ca. 26 nm, attributed to the micelles. The distribution of the unimers disappeared at Pf-11/PySt = 3.0, indicating that the micellization was completed.

^{1}H NMR revealed that the micellization occurred through the salt formation between the pyridine moiety and the perfluoroalkyl carboxylic acid. Figure 5 shows the ^{1}H NMR spectra obtained for the PPySt-*b*-PSt copolymer at each Pf-11/PySt molar ratio in THF-d_8. As the Pf-11/PySt ratio increased, the signals at 7.18 and 8.40 ppm for the aromatic protons of the pyridine rings were broadened much more and were shifted to a lower magnetic field side. The signals at 4.40 ppm for two methylenes were also broadened and were shifted to a lower magnetic field side. The signals were divided into two as the micellization proceeded. The signals observed at a higher magnetic field should originate from the

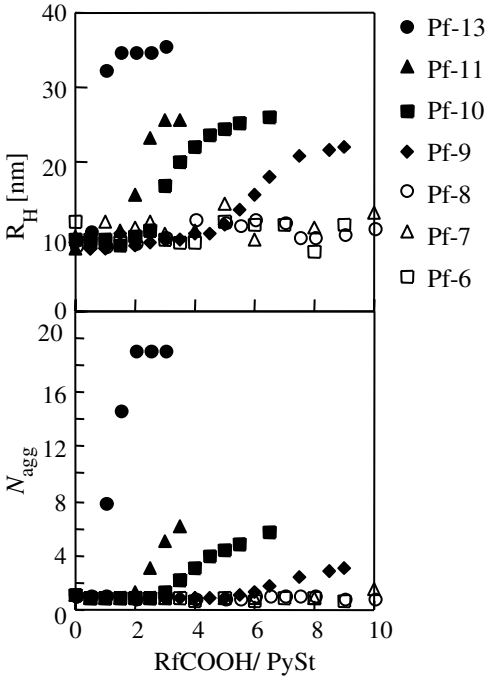

Fig. 3 Variation in the hydrodynamic radius and the aggregation number of the PPySt-*b*-PSt copolymer through the micellization using Pf-6, Pf-7, Pf-8, Pf-9, Pf-10, Pf-11, and Pf-13. [copolymer] = 3.33×10^{-3} g/mL. Solvent: THF. Temperature: 20 °C

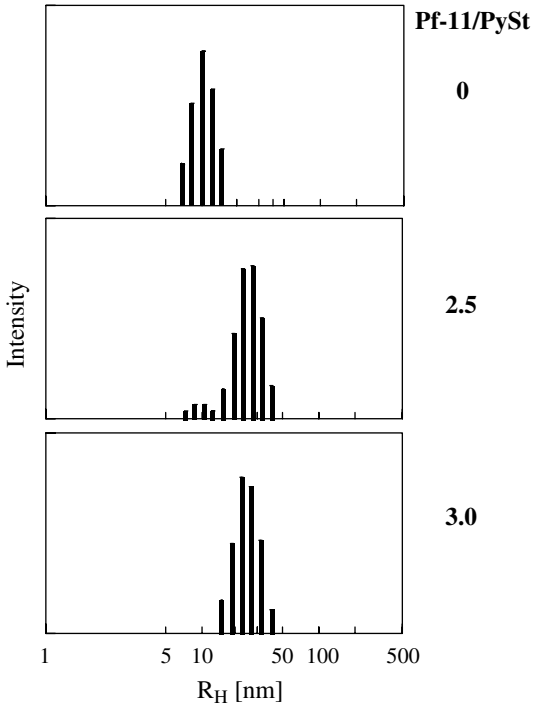

Fig. 4 Variation in the intensity distribution of the hydrodynamic radius of the PPySt-*b*-PSt copolymer through the micellization using Pf-11. [copolymer] = 3.33×10^{-3} g/mL

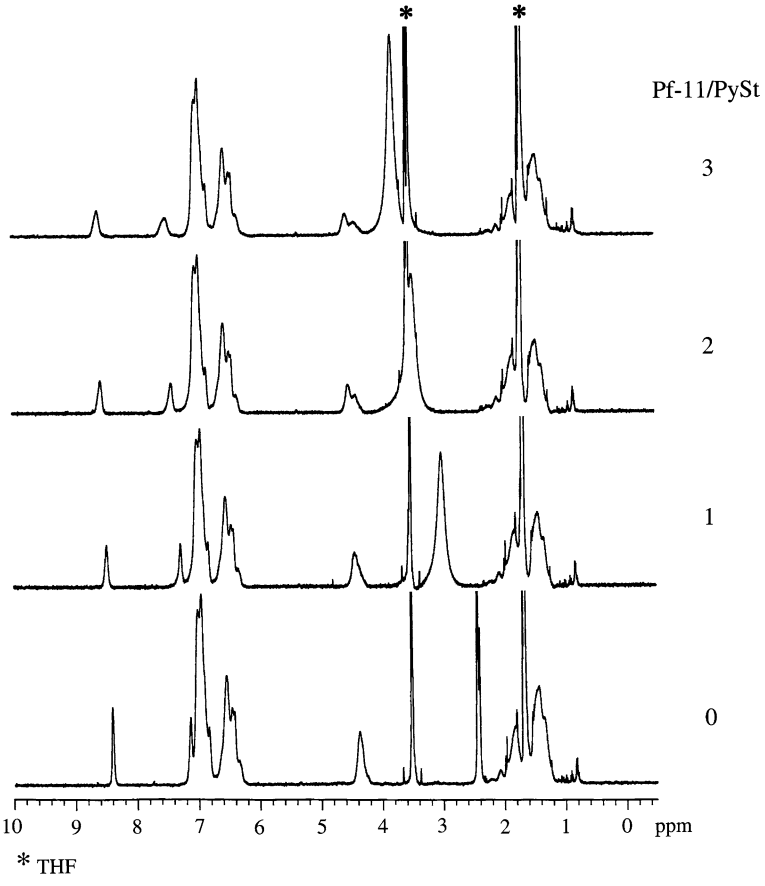

Fig. 5 ^{1}H NMR spectra of PPySt-*b*-PSt in the micellization by Pf-11 at 20 °C. Solvent: THF-d_8. [copolymer] = 3.33×10^{-3} g/mL

methylene attached to the pyridine ring, while the signals at a lower magnetic field from the benzyl group.

The shifts of the signals to a lower magnetic field were also observed by the addition of Pf-8 to the copolymer solution. Pf-8 formed the salt with the pyridine moiety. However, the copolymer produced no micelles in the presence of Pf-8, as a result the signals of the pyridine moieties were less broadened by Pf-8 in comparison with the signals broadened by Pf-11. On the other hand, in the micelle formation by Pf-13, the signals at 4.40, 7.18, and 8.40 ppm were slightly observed. The strong aggregation force of the long perfluoroalkyl chains in Pf-13 produced the micelles with the tight cores.

We explored the temperature-dependence of the micelle formation using Pf-11. The micellization was performed at 10, 20, 30, and 40 °C. Figure 6 shows the variability in the hydrodynamic radius of the copolymer and the aggregation number through the micellization at each temperature. The transition from the unimers to the micelles was shifted to the higher side of the Pf-11/PySt ratio as a result of increasing temperature. The aggregation number at complete micellization decreased with an increase in the temperature, while the hydrodynamic radius of the micelles was almost independent

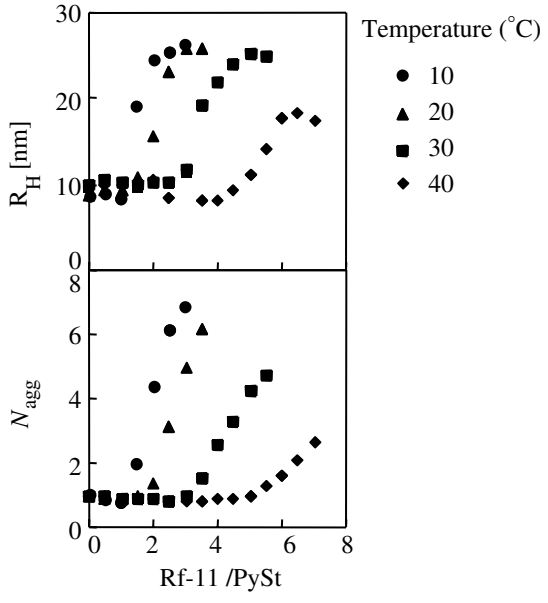

Fig. 6 Variability in the hydrodynamic radius of the PPySt-*b*-PSt copolymer and the aggregation number through the micellization by Pf-11 at each temperature. [copolymer] = 3.33×10^{-3} g/mL

of the temperature (R_H = ca. 26 nm) with the exception of that at 40 °C. The hydrodynamic radius of the micelles prepared at 40 °C was ca. 18 nm. The formation of the smaller size of the micelles at 40 °C should be due to the smaller aggregation number of ca. 3. The increase in the temperature weakens the aggregation force among the perfluoroalkyl chains, resulting in the formation of the micelles with a low aggregation number and high critical temperature.

The thermostability of the PPySt-*b*-PSt micelles was investigated by the NNLS analysis. The micellar solution prepared at 10 °C with Pf-11 (Pf-11/PySt = 3.5) was subjected to this study. The variation in intensity distribution of the hydrodynamic radius of the copolymer is shown in Fig. 7. Only the distribution of the micelles was observed at 10 °C. When the temperature increased to 20 °C, the distribution of the unimers was discerned in addition to that of the micelles. The intensity of the unimer distribution increased instead of a decrease in the micellar distribution. At 40 °C, only the unimer distribution was observed. The micelles were dissociated into the unimers by increasing the temperature.

Figure 8 shows the variation in the hydrodynamic radius and the aggregation number with the changes in the temperature. The micellar solution prepared at 10 °C with Pf-11 (Pf-11/PySt = 3.5) was heated up to 40 °C, then it was cooled down to 10 °C. The hydrodynamic radius of the copolymer decreased as the temperature increased. This decrease in the hydrodynamic radius is based not on contraction of the micelles but on the estimation as an average of the hydrodynamic radii for the micelles and the unimers in the proportion of existence at each temperature. The aggregation number also decreased as the temperature increased. At 40 °C the hydrodynamic radius of the copolymer was equal to that of the unimer, when the aggregation number reached 1. The micelles were dissociated into the unimers by increasing the temperature. When the temperature decreased, the hydrodynamic radius and the aggregation number increased, following almost the same loci as those for the temperature increased. The hydrodynamic radius and the aggregation number reverted to the initial values at 10 °C. The micelles were reconstructed by decreasing the temperature. This good hysteresis indicates that the dissociation–reconstruction of the micelles is reversibly controlled by the temperature (Fig. 9).

The Pf-11 concentration manipulated the dissociation–reconstruction of the micelles. Figure 10 shows the hysteresis curves obtained for the micelles prepared at Pf-11/PySt = 7.0. The micelles showed good hysteresis for the variation in temperature, as did the micelles at Pf-11/PySt = 3.5. The hysteresis curves, however, were shifted to a higher side of the temperature. As a result of increasing the Pf-11 concentration, the micelles were

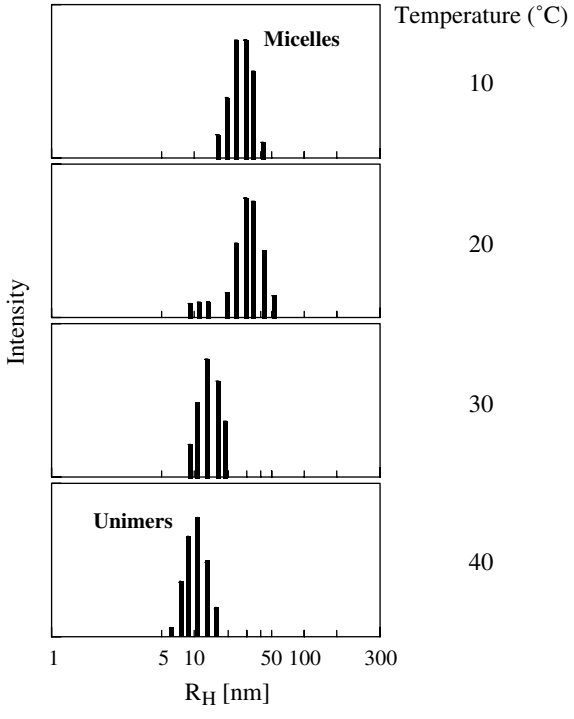

Fig. 7 Intensity distribution of the PPySt-*b*-PSt micelles at each temperature. Pf-11/PySt = 3.5. [copolymer] = 3.33×10^{-3} g/mL

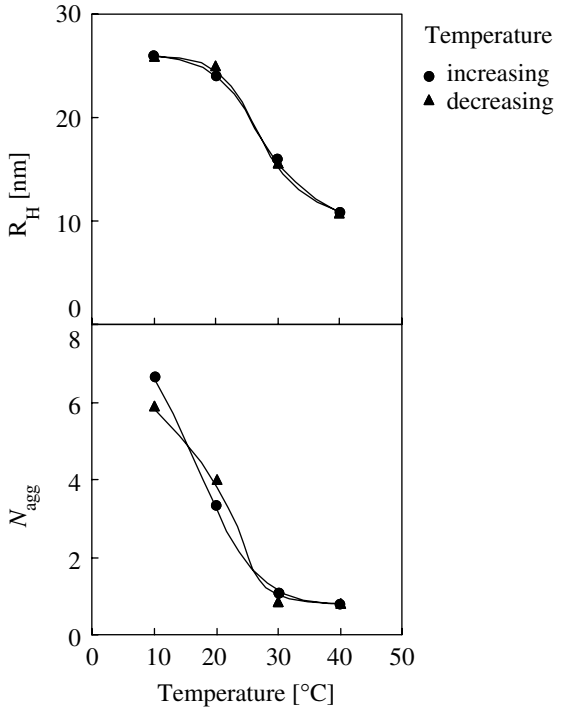

Fig. 8 Hysteresis curves of the PPySt-*b*-PSt micelles with Pf-11 for the temperature. Pf-11/PySt = 3.5. [copolymer] = 3.33×10^{-3} g/mL

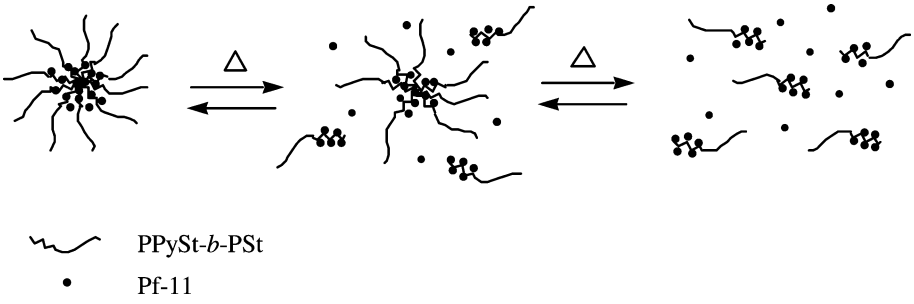

Fig. 9 Dissociation–reconstruction of the PPySt-*b*-PSt micelles with Pf-11 by the changes in the temperature

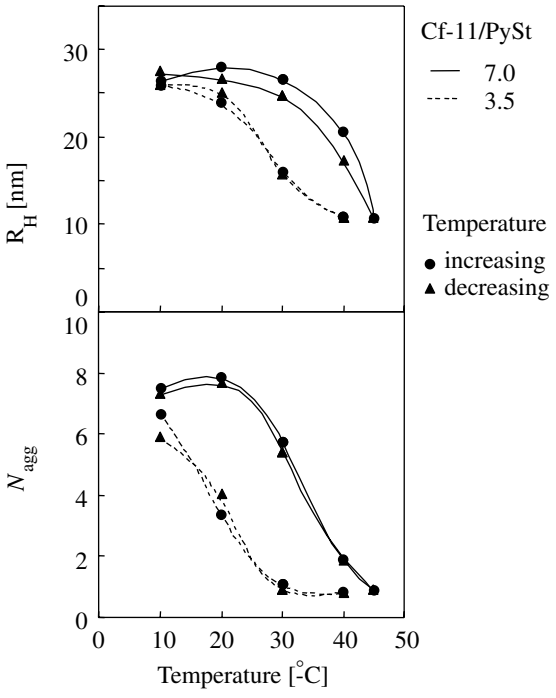

Fig. 10 Hysteresis curves of the PPySt-*b*-PSt micelles at different Pf-11/PySt ratios for the temperature. [copolymer] = 3.33×10^{-3} g/mL

more difficult to dissociate into the unimers, while the micelles were easier to reconstruct. The Pf-11/PySt ratio can also control the dissociation–reconstruction of the micelles reversibly.

Conclusion

The PPySt-*b*-PSt copolymer formed the micelles in the nonselective solvent in the presence of the perfluoroalkyl carboxylic acids with long perfluoroalkyl chains. The micellization proceeded through the salt formation of the pyridinium perfluoroalkyl carboxylate and through the aggregation among the prefluoroalkyl chains. The length of the perfluoroalkyl chain not only dominated the self-assembly of the copolymer, but also determined the micellar size and the aggregation number. The micellization by the perfluoroalkyl carboxylic acid showed temperature-dependence. The copolymer needed more perfluoroalkyl carboxylic acid at higher temperature to produce the micelles. The copolymer formed the micelles with lower aggregation number at higher temperature, although the micellar size was almost independent of the temperature. The micelles were dissociated into the unimers by increasing the temperature, and were reconstructed by decreasing it. The dissociation–reconstruction of the micelles was reversibly controlled by the variation in the temperature. The concentration of the perfluoroalkyl carboxylic acid also manipulated the dissociation–reconstruction reversibly. An increase in the acid concentration suppressed the dissociation of micelles, while promoting their reconstruction.

This is the first light scattering study demonstrating that the length of the perfluoroalkyl chain as the counter anions manipulated the hydrodynamic radius, the aggregation number, the critical micelle concentration, and the thermal response of the micelles.

References

1. Neradovic D, Nostrum CF, Hennink WE (2001) Macromolecules 34:7589
2. Arotcarena M, Heise B, Ishaya S, Laschewsky A (2002) J Am Chem Soc 124:3787
3. Lowe AB, Billingham NC, Armes SP (1997) Chem Commun 1035
4. Weaver JVM, Armes SP, Butun V (2002) Chem Commun 2122
5. McClain JB, Canelas DA, Samulski ET, DeSimone JM, Londono JD, Cochran HD, Wignall GD, Chillura-Martino GD, Triolo R (1996) Science 274:2049
6. Buhler E, Dobrynin AV, DeSimone JM, Rubinstein M (1998) Macromolecules 31:7347
7. Zhou S, Chu B (1998) Macromolecules 31:5300
8. Celso L, Triolo A, Triolo F, Donato DI, Steinhart M, Kriechbaum M, Amenitsch H, Triolo R (2002) Eur Phys J (2002) Soft Matter 8:311
9. Koga T, Zhou S, Chu B (2001) Appl Opt 40:4170
10. Lee AS, Butun V, Vamvakaki M, Armes S, Pople JA, Gast AP (2002) Macromolecules 35:8540

11. Liu S, Weaver JVM, Tang Y, Billingham NC, Armes SP (2002) Macromolecules 35:6121
12. Hu Y, Kramer MC, Boudreaux CJ, McCormick CL (1995) Macromolecules 28:7100
13. Chernyshov DM, Bronstein LM, Boerner H, Berton B, Antonietti M (2000) Chem Mater 12:114
14. Liu S, Zhu H, Zha H, Jiang M, Wu C (2000) Langmuir 16:3712
15. Harada A, Kataoka K (1995) Macromolecules 28:5294
16. Martin TJ, Prochazka K, Munk P, Webber SE (1996) Macromolecules 29:6071
17. Gohy J-F, Lohmeijer GG, Varshney SK, Decamps B, Leroy E, Boileau S, Schubert US (2002) Macromolecules 35:9748
18. Liu S, Zhang G, Jiang M (1999) Polymer 40:5449
19. Gohy J-F, Varshney SK, Jerome R (2001) Macromolecules 34:3361
20. Brontein LM, Sidorov SN, Valetsky PM (1999) Langmuir 15:6256
21. Zhao H, Douglas EP (2002) Mater Res Soc Symp Proc 43
22. Miyazawa T, Endo T, Shiihashi S, Okawara M (1985) J Org Chem 50:1332
23. Morrison ID, Grabowski EF, Herb CA (1985) Langmuir 1:496